

COMPUTER SIMULATION OF CRYSTAL NUCLEATION OF PARALLEL HARD SPHEROCYLINDERS

J.A.C. VEERMAN and D. FRENKEL

*F.O.M.-Institute for Atomic and Molecular Physics, P.O. Box 41883, 1009 DB Amsterdam,
The Netherlands*

Received 4 November 1988

We report a molecular dynamics study of homogeneous nucleation in a fluid of parallel hard spherocylinders. It is found that the rate of nucleation of the crystal depends strongly on the presence of a nearby metastable smectic phase.

1. Introduction

In 1897 Ostwald [1] observed that homogeneous nucleation proceeds according to the following rule: *When a transition from one phase to a more stable phase occurs, the latter phase will not be the one that is most stable under the given circumstances, but the phase that is closest in free energy to the initial one.*

In 1978, Alexander and McTague [2] argued on basis of Landau theory that for systems of particles with a spherically symmetric potential, the initial crystalline nucleus should preferentially have a bcc structure, even if other structures are thermodynamically more stable. Although homogeneous nucleation in atomic fluids has been studied extensively by computer simulation by a number of authors [3, 4], the numerical evidence to support the Alexander–McTague conjecture is less than conclusive.

To our knowledge, no numerical studies of homogeneous nucleation on systems of non-spherically symmetric particles have been performed so far. In the present article we present the results of a Molecular Dynamics (MD) study on homogeneous nucleation on a system of parallel hard spherocylinders. A spherocylinder consists of a cylindrical segment of length L and diameter D capped at each end by a hemisphere of the same diameter. The phase diagram of this model for various values of L/D has been reported by Stroobants et al. [5] (fig. 1). For $L/D < 0.5$ the low-density “nematic” phase exhibits a first order freezing transition. For $0.5 < L/D < 3$ the translational ordering proceeds in steps: as the fluid is compressed to a density ρ_{NS} the low density

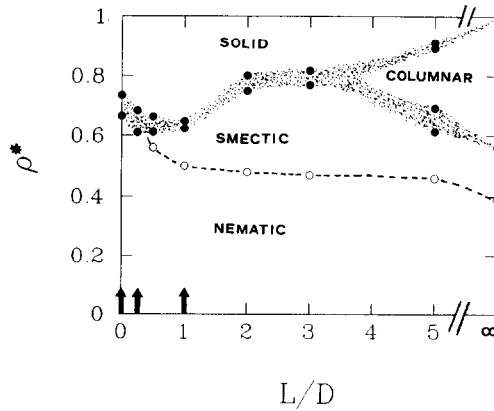


Fig. 1 (ref. [5]). Phase diagram of hard parallel spherocylinders as a function of the length-to-width ratio L/D . The shaded areas correspond to two-phase regions. Black circles, densities of the coexisting phases; open circles, densities corresponding to the continuous nematic–smectic and smectic–columnar transitions. The arrows denote the L/D -values at which the nucleation studies were performed.

nematic phase transforms into a smectic-A phase. The latter undergoes a first-order freezing transition at a higher density ρ_{SC} . For all L/D values the freezing transition is strongly first order: on freezing there is a discontinuity in the density of some 10%.

The reason why it is interesting to study nucleation in this system is that it offers the possibility to study the competition between nucleation into a thermodynamically stable crystal phase and the formation of a (metastable) smectic phase.

The remainder of this paper is organized as follows: in section 2 we describe the simulation techniques used to prepare the system in a non-equilibrium phase and study its time evolution. In section 3 we discuss the quantities used to monitor the nucleation process, while in section 4 the results of the calculations are presented. In section 5 we discuss some of the implications of our results.

2. Simulation technique

Before discussing our simulation procedure, a general remark is in place. The present paper discusses nucleation in a rather small ($N = \mathcal{O}(10^2)$) model system with periodic boundary conditions. It is well known that the rate of “homogeneous” nucleation of such a model system may depend strongly on the system size. The work of Honeycutt and Andersen [6] showed that, due to

periodic boundary conditions, nucleation occurs much faster when the system size is small. The obvious method to eliminate this problem is to carry out simulations in a larger system. Of course, the price that must be paid when studying nucleation in a system that is sufficiently large to suppress finite-size effects is a larger expenditure of computer time. In the present simulations we considered it preferable to spend the available computer time on a comparative numerical study of a set of different model systems of only a few hundred particles, rather than on one or two runs on a very large system. As a consequence, not too much significance should be attached to the absolute nucleation rates found in the present work. However, the present study should yield a meaningful comparison of relative nucleation rates in different model systems.

A simulation on the spherocylinder system was performed as follows: an equilibrium fluid of 288 or 270 particles at a density just below the coexistence region was compressed by means of a constant pressure Monte Carlo (MC) program to a density within the coexistence region. Subsequently, the system was allowed to evolve by means of the conventional constant-volume “hard core” MD method [7]. Typically a MC compression from a reduced density (i.e. the density relative to the closest packing density) $\rho^* = 0.60$ to $\rho^* = 0.66$ took about 1800 MC cycles, which proved to be fast enough to leave the system in an essentially disordered state (i.e. a state with no long-range translational order (viz. fig. 4)). The MD run lasted 300 time-units, where one time-unit is given by the quantity $D\sqrt{m/kT}$, with D the particle diameter and m the mass of the particle. During a run each particle experienced about 6000 collisions.

3. Analysis of time evolution

During a run we studied the time evolution of a number of thermal, dynamical and structural properties of the system. For these purposes we used the following quantities:

1. Thermal

- The compressibility factor

$$\Pi^* = PV/NkT - 1. \quad (1)$$

When the system is in equilibrium Π^* will perform small fluctuations about its equilibrium value. When nucleation occurs, Π^* will decrease until it reaches a value that corresponds to a (possibly defect-rich) crystalline solid.

2. Dynamical

– Mean square displacement $\langle R^2(t) \rangle$. We used this quantity to measure the diffusion in the system. In order to discern between diffusion parallel and perpendicular to the alignment of the cylinders we made a division into

$$\langle R_{\parallel}^2(t) \rangle = N^{-1} \sum_j (r_{\parallel j}(t) - r_{\parallel j}(0))^2 \quad (2)$$

and

$$\langle R_{\perp}^2(t) \rangle = N^{-1} \sum_j (r_{\perp j}(t) - r_{\perp j}(0))^2. \quad (3)$$

Here $\langle R_{\parallel}^2(t) \rangle$ and $\langle R_{\perp}^2(t) \rangle$ are the mean square displacements parallel and perpendicular to the alignment of the spherocylinders. By studying these quantities we can also draw some conclusions about the structure of the system: in a nematic phase (which is the most disordered phase of the present model system) both $\langle R_{\parallel}^2(t) \rangle$ and $\langle R_{\perp}^2(t) \rangle$ will increase linearly in time. In a smectic phase $\langle R_{\parallel}^2(t) \rangle$ will only increase very slowly, while in a solid phase both $\langle R_{\parallel}^2(t) \rangle$ and $\langle R_{\perp}^2(t) \rangle$ will remain constant (apart from small fluctuations).

3. Structural

– Structure factors $S(\mathbf{k})$. We considered the structure factors at two values of the wavevector \mathbf{k} , namely the maximum structure factor in the z -direction,

$$S_m(\mathbf{k}_{\parallel}) = \max_{k_{\parallel}} N^{-1} \left| \sum_j \exp i\mathbf{k}_{\parallel} \cdot \mathbf{r}_j \right|^2, \quad (4)$$

and the maximum structure factor in the xy -plane,

$$S_m(\mathbf{k}_{\perp}) = \max_{k_{\perp}} N^{-1} \left| \sum_j \exp i\mathbf{k}_{\perp} \cdot \mathbf{r}_j \right|^2. \quad (5)$$

Here, and in the following equations, the z -axis is chosen parallel to the alignment of the cylinders, which is also the orientation of one of the box axes. The x - and y -axes are chosen parallel to the other two box axes. The \mathbf{k} -vectors for which the maxima were obtained were also recorded. Thus we obtained a measure for the periodicity in the system both in the z -direction and perpendicular to the z -direction.

Using the “parallel” structure factor (eq. (4)) a nematic phase can easily be discerned from a smectic phase. In order to discern a smectic phase from an anharmonic solid phase we can use the transverse structure factor (eq. (5)).

However, it is often more convenient to monitor the onset of in-plane crystalline order by looking at the in-plane bond order. We therefore introduced the following order parameters:

– Bond order parameters ψ_6^2, χ_6^2 . We define ψ_6^2 by

$$\psi_6^2 = \frac{\left| \sum'_{i<j} \exp 6i\theta_{ij} \right|^2}{\left| \sum'_{i<j} \exp 6i\theta_{ij}^{id} \right|^2}. \tag{6}$$

Here θ_{ij} is the angle between the projection of r_{ij} on the xy -plane and the x -axis, and the sum is taken over all pairs of particles for which

$$r_{\parallel ij} < 0.7r_{\parallel nn}, \quad r_{\perp ij} < 1.35r_{\perp nn}. \tag{7}$$

Here $r_{\parallel nn}$ and $r_{\perp nn}$ are the parallel and perpendicular distances between nearest neighbours in a perfect (“stretched fcc”) lattice at the same density as the system under consideration. The factor 1.35 is chosen in such a way that the cutoff is about halfway between the nearest and next-nearest neighbours within one layer. The sum in the denominator is the same as the sum in the numerator, but evaluated for a perfect lattice. For a system of N particles it is given by

$$\left| \sum_{i<j} \exp 6i\theta_{ij}^{id} \right|^2 = 9N^2. \tag{8}$$

By construction $\psi_6^2 = 1$ for a perfect lattice, while for a completely disordered (e.g. nematic) fluid $\psi_6^2 = \mathcal{O}(1/N)$. It is also useful to measure bond order in a smectic phase within each layer separately. We therefore introduced a bond order parameter for smectic layers:

$$\chi_6^2 = (3N_l)^{-2} \left| \sum''_{i<j} \exp 6i\theta_{ij} \right|^2. \tag{9}$$

Here the sum is taken over all pairs within a smectic layer, and N_l is the number of particles of the layer. We also introduced the mean angle of bond order within a smectic layer by

$$\theta_m = \frac{1}{6} \arctan \frac{\text{Im} \left(\sum''_{ij} \exp 6i\theta_{ij} \right)}{\text{Re} \left(\sum''_{ij} \exp 6i\theta_{ij} \right)}. \tag{10}$$

Knowledge of this quantity for all smectic layers allows us to detect possible correlations in bond order between the smectic layers.

Beside the study of the above-mentioned parameters, we found it extremely useful to gain an indication of the state of the system by studying snapshots of the molecular configuration at regular intervals during a run.

4. Simulation results

We performed a total of 10 simulations on three different systems. The first ($L/D = 0$) corresponds to the well-known hard sphere system which has no smectic phase. The second ($L/D = 0.25$) has no thermodynamically stable

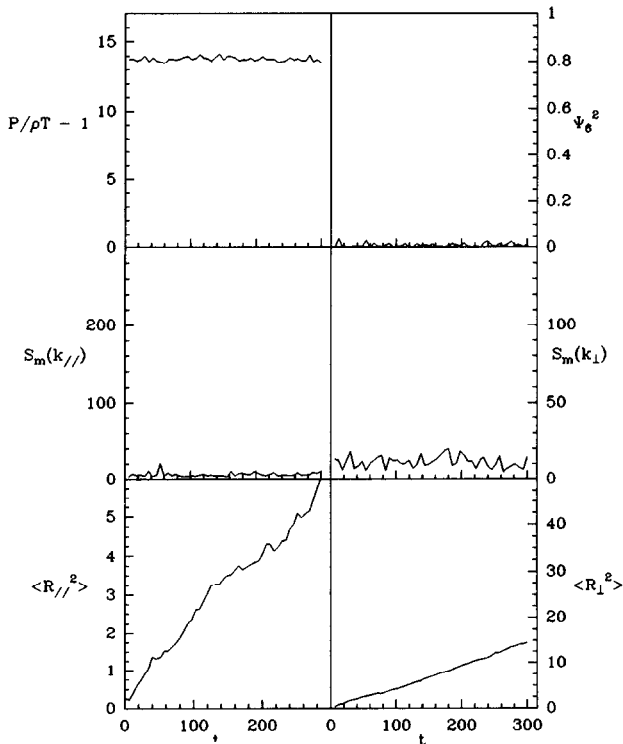


Fig. 2. Measured quantities for $L/D = 0$ (hard spheres). $P/\rho T - 1$ is the compressibility factor (the Boltzmann constant $k = 1$ in this figure), ψ_6^2 is the bond order parameter defined by eq. (6), $S_m(k_{||})$ and $S_m(k_{\perp})$ are the maximum structure factors defined by eqs. (4) and (5), and $\langle R_{||}^2 \rangle$ and $\langle R_{\perp}^2 \rangle$ are the mean square displacements defined by eqs. (2) and (3), measured in units D^2 , where D is the diameter of the cylinder.

smectic phase, but it may have a metastable smectic phase at a density above the freezing point [8]. The third ($L/D = 1$) has a stable smectic-A phase [5]. As independent simulations of the same state points showed essentially identical behaviour we only present the results of one run per state point.

Below we briefly summarize the main results of our numerical study:

1. $L/D = 0$ (hard spheres) (288 particles, liquid-solid coexistence region: $\rho^* = 0.67-0.74$ [9])

– $\rho^* = 0.70$ (fig. 2). This is a density well inside the coexistence region between solid and liquid. The results are given in fig. 2. The fluctuations in Π^* are small and the diffusion coefficients (which directly follow from the time derivative of the mean square displacements) are approximately constant, and show isotropy in the diffusion. All structural order parameters remain small. We can conclude that the system remains in its metastable fluid phase.

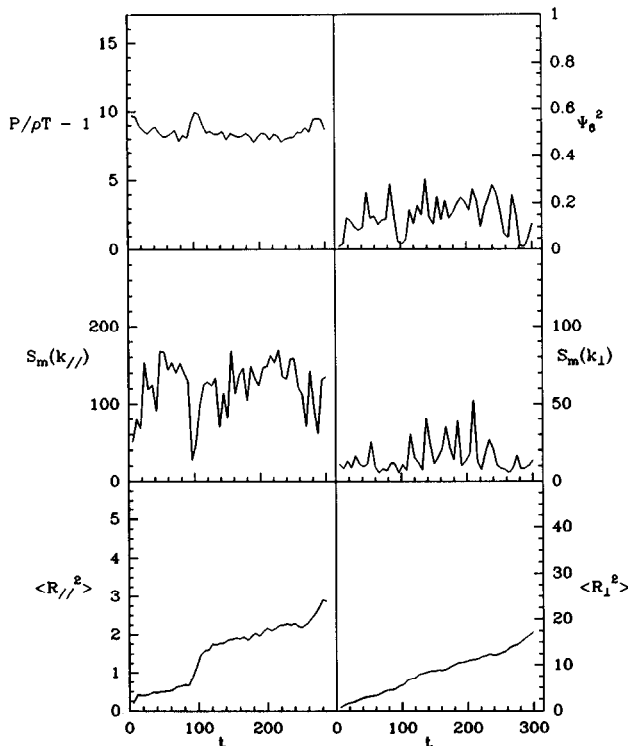


Fig. 3. Same as in fig. 2, but for $L/D = 0.25$, $\rho^* = 0.63$. Note that this density corresponds to a point in the solid-liquid coexistence region, close to the liquid branch.

2. $L/D = 0.25$ (288 particles, nematic-solid coexistence region: $\rho^* = 0.610\text{--}0.685$ [5])

– $\rho^* = 0.63$. (figs. 3, 4). This is a density at the lower end of the coexistence region. We see strong fluctuations in Π^* and ψ_6^2 , with ψ_6^2 small when Π^* is large, and vice versa. We can also observe some correlation between the behaviour of $S_m(\mathbf{k}_\perp)$ and Π^* (see e.g. the “dip” at $t = 100$). The behaviour of $\langle R_{\parallel}^2(t) \rangle$ shows that the diffusion parallel to the spherocylinder alignment slows down when Π^* is small, while no significant change in behaviour of $\langle R_{\perp}^2(t) \rangle$ can be observed. Snapshots show that smectic-like ordering coincides with low values of Π^* . Fig. 4 shows that the system is fluctuating between a nematic and a smectic phase. Measurements of χ_6^2 indicate that local solidlike ordering occurs occasionally (once in a run of $t = 300$).

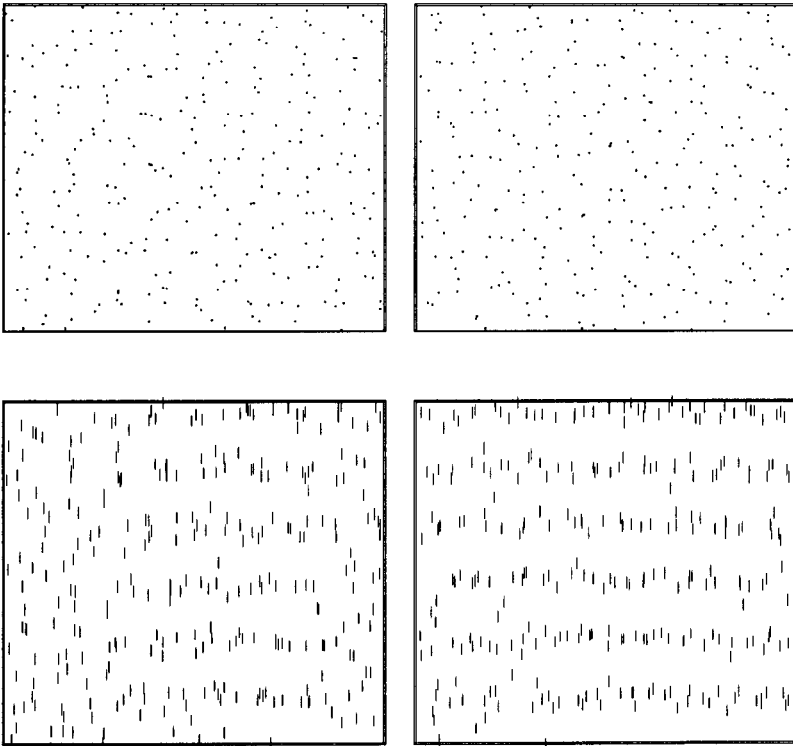


Fig. 4. Particle configurations for $L/D = 0.25$, $\rho^* = 0.63$ at $t = 0$ (i.e. immediately after compression) (left) and $t = 300$ (right). The upper pictures show a projection in the plane perpendicular to the molecular axis; the lower pictures show a projection in the plane parallel to the direction of alignment. The spherocylinders are indicated by a line segment of length L . Note that there are already smectic fluctuations present in the initial configuration. These are however not larger than the smectic precursor fluctuations, which appear in the nematic fluid at a density just below the coexistence region [11].

– $\rho^* = 0.66$ (table I, figs. 5, 6). This is a density at the upper end of the coexistence region. Here we see a sharp drop in Π^* until $t \approx 20$, after which it remains constant. ψ_6^2 increases rapidly and remains constant also after $t \approx 20$. The structure factors $S_m(\mathbf{k}_{\parallel})$ and $S_m(\mathbf{k}_{\perp})$ also become large. Both $\langle R_{\perp}^2(t) \rangle$ and $\langle R_{\parallel}^2(t) \rangle$ remain small, and show no increase after $t \approx 20$. χ_6^2 is large after $t \approx 20$, and snapshots show a clear solid structure. It is clear that a rapid nucleation to a solid-state structure has occurred.

3. $L/D = 1$ (270 particles, smectic-solid coexistence region: $\rho^* = 0.624\text{--}0.650$ [5])

– $\rho^* = 0.63$ (table II, figs. 7, 8). We see Π^* decreasing continually, while ψ_6^2 and $S_m(\mathbf{k}_{\perp})$ remain small all the time. $S_m(\mathbf{k}_{\parallel})$ is large all the time, except for a dip at $t \approx 260$. $\langle R_{\parallel}^2(t) \rangle$ and $\langle R_{\perp}^2(t) \rangle$ increase slowly until $t \approx 260$. At $t \approx 260$ $\langle R_{\perp}^2(t) \rangle$ shows a rapid increase coinciding with the dip in $S_m(\mathbf{k}_{\parallel})$. The behaviour of χ_6^2 shows an increase in sixfold symmetry with increasing time. Snapshots of the smectic layers confirm this. From $6\theta_m$ it can be seen that there

Table I

Bond order results for $L/D = 0.25$. ρ^* is the reduced density, t is the time at which χ_6^2 is determined. z_{mean} is the mean coordinate of the particles within a smectic layer, χ_6^2 is the structural order parameter determined by eq. (9), N_l is the number of particles in a smectic layer and θ_m is the mean bond order angle determined by eq. (10).

ρ^*	t	z_{mean}	χ_6^2	N_l	θ_m
0.66	0	-2.91	0.126	49	-6.78°
		-1.64	0.153	48	-12.39°
		-0.45	0.042	46	-12.85°
		0.76	0.031	49	12.81°
		1.96	0.086	44	-1.43°
		3.18	0.061	52	-9.44°
	30	-2.78	0.48	48	-0.06°
		-1.55	0.29	49	-0.65°
		-0.33	0.50	48	0.12°
		0.86	0.40	47	0.49°
		2.11	0.54	48	-0.00°
		3.33	0.64	48	0.09°
	300	-2.79	0.57	48	-0.08°
		-1.56	0.58	48	0.07°
		-0.36	0.59	48	-0.04°
0.85		0.41	48	0.63°	
2.09		0.57	48	-0.03°	
3.34		0.59	48	0.16°	

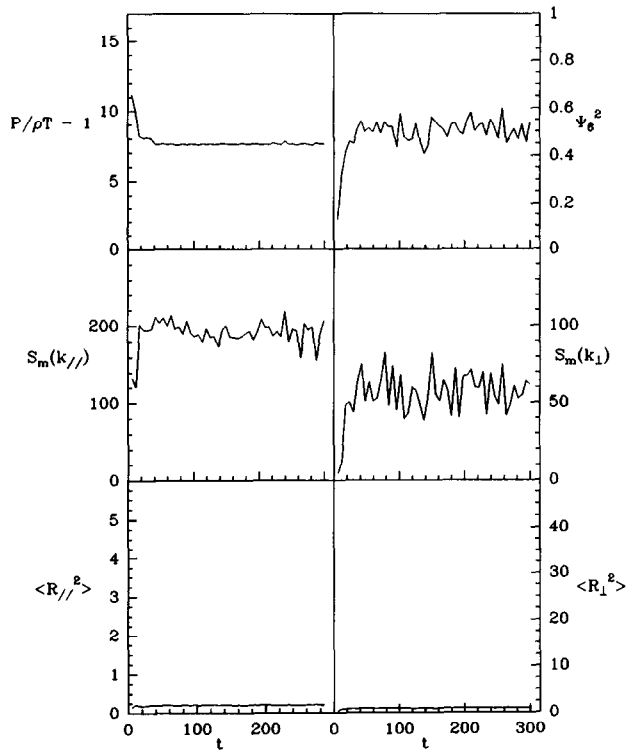


Fig. 5. Same as in fig. 2, but for $L/D = 0.25$, $\rho^* = 0.66$. Note that this is a density close to the solid branch.

is no clear correlation in bond order between the various smectic layers, which explains why ψ_6^2 remains small. The behaviour of $S_m(k_{\parallel})$, and $\langle R_{\perp}^2(t) \rangle$ at $t \approx 260$ may be caused by the motion of a defect in the layer structure.

- $\rho^* = 0.64$. Here we see essentially the same behaviour as for $\rho^* = 0.63$, with however somewhat more solid ordering at the end of the run.

5. Discussion and conclusions

Comparing the $L/D = 0$ run with the $L/D = 0.25$ runs, we see that a small change in particle shape brings about an enormous change in the nucleation rate. While the hard-sphere system shows no nucleation at all anywhere within the coexistence region (nucleation appears to be possible, but only at a density

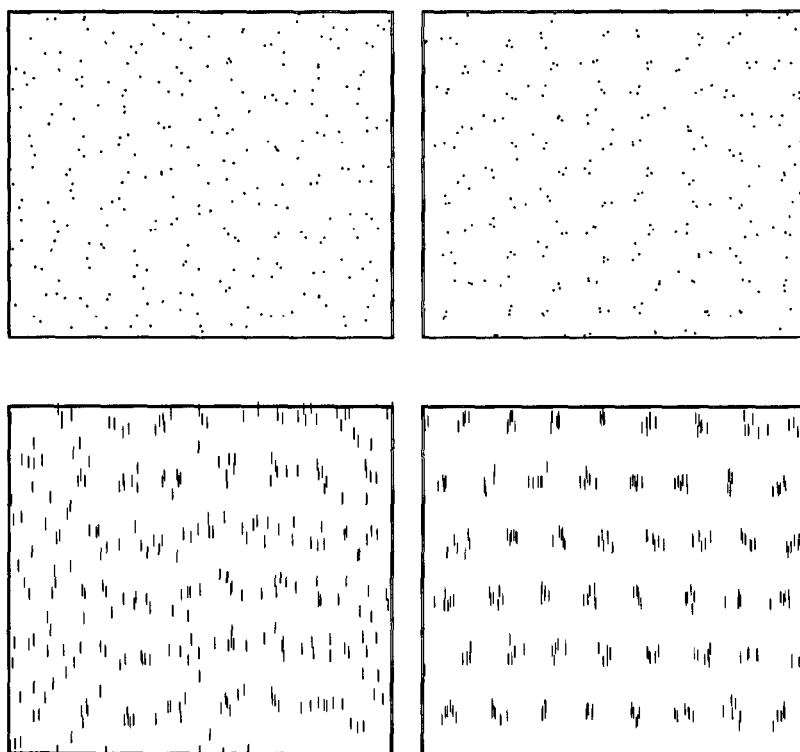


Fig. 6. Same as in fig. 4, but for $L/D = 0.25$, $\rho^* = 0.66$.

well above the coexistence region [10]), nucleation occurs easily within the coexistence region for the $L/D = 0.25$ system. The $\rho^* = 0.63$ run showed that in this process a smectic phase is involved. The computations of ref. [5] showed that this smectic phase can only be metastable. The behaviour of the $L/D = 0.25$ system is thus in accordance with Ostwald's rule. The latter rule "explains" why nucleation occurs more easily than for the hard-sphere system: the presence of a metastable smectic phase lowers the free energy barrier between nematic and solid state (fig. 9). In a hard sphere system such a metastable state is not present.

It should be noted that the behaviour observed in the present simulations is, in fact, slightly different from that exhibited by the experimental systems to which Ostwald's rule was applied originally. In the latter systems the phase transformation occurs through nucleation, whereas the nematic-smectic transi-

Table II

Same as in table I, but for $L/D = 1$.

ρ^*	t	z_{mean}	χ_6^2	N_i	θ_m
0.63	0	-8.41	0.098	29	4.27°
		-6.37	0.154	30	14.45°
		-4.30	0.076	29	11.38°
		-2.20	0.076	31	-12.94°
		-0.07	0.094	29	10.20°
		2.00	0.091	29	-10.23°
		4.08	0.066	31	6.52°
		6.17	0.059	31	3.81°
		8.25	0.039	31	2.95°
		216		-8.43	0.283
-6.36	0.096			30	-1.58°
-4.31	0.118			30	0.26°
-2.26	0.023			30	5.74°
-0.15	0.195			30	8.19°
1.93	0.066			30	-6.35°
4.09	0.020			30	-13.79°
6.14	0.155			31	-13.56°
8.21	0.064			29	-13.54°
300		-8.44	0.333	30	0.60°
		-6.34	0.062	30	-8.78°
		-4.26	0.016	29	-3.72°
		-2.13	0.204	30	0.93°
		-0.05	0.162	30	5.50°
		1.97	0.264	30	-2.52°
		4.02	0.311	30	-0.51°
		6.10	0.252	31	-4.59°
		8.21	0.165	30	0.64°

tions in hard parallel spherocylinders appears to be continuous or weakly first order. Hence the phase transformation to the metastable smectic phase proceeds with little if any nucleation barrier. This is also the reason why some smectic order is already present in the $L/D = 0.25$ system immediately after compression (figs. 4, 6): it takes a finite amount of time to compress a system of hard particles to the desired "metastable" density. Due to the absence of a nucleation barrier the onset of smectic ordering starts already during the compression.

For the $L/D = 1$ system the nucleation process proceeds much more slowly than for the $L/D = 0.25$ system but, in contrast to the hard sphere system, order is developing. Apparently crystallisation from a metastable smectic phase is easier for $L/D = 0.25$ than for $L/D = 1$. Why this should be so is not clear at present.

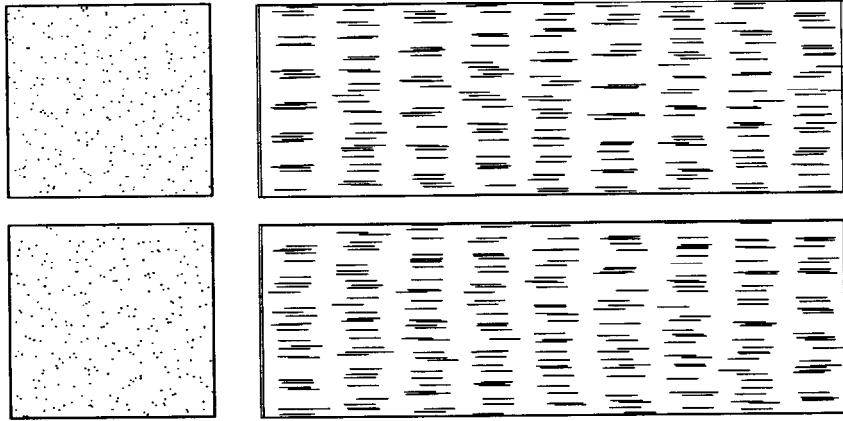


Fig. 8. Same as in fig. 4, but for $L/D = 1$, $\rho^* = 0.63$.

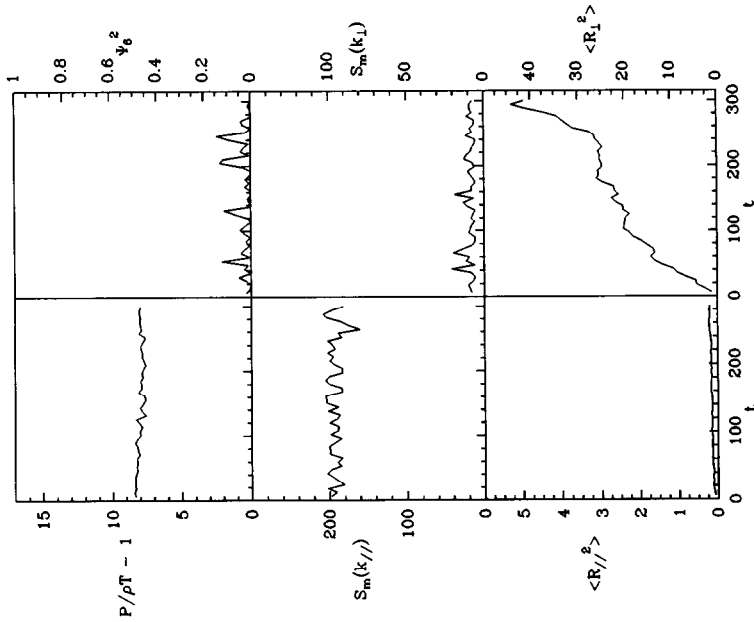


Fig. 7. Same as in fig. 2, but for $L/D = 1$, $\rho^* = 0.63$.

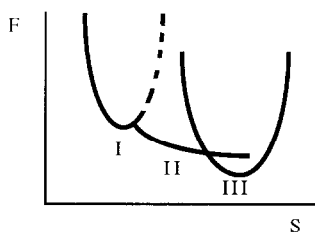


Fig. 9. Schematic drawing of the free energy of a system of hard parallel spherocylinders as a function of a characteristic crystalline order parameter S at a density where the crystalline phase is the more stable. I is the nematic branch, II the smectic branch and III the solid branch. The presence of the smectic branch lowers the nucleation barrier.

Acknowledgements

This work is part of the research program of the Stichting voor Fundamenteel Onderzoek der Materie (Foundation for Fundamental research on Matter) and was made possible by financial support from the Nederlandse Organisatie voor Wetenschappelijk Onderzoek (Netherlands Organization for the Advancement of Research).

References

- [1] W. Ostwald, *Z. Phys. Chem.* 22 (1897) 289.
- [2] S. Alexander and J. McTague, *Phys. Rev. Lett.* 41 (1978) 702.
- [3] J.N. Cape, J.L. Finney and L.V. Woodcock, *J. Chem. Phys.* 75 (1981) 2366.
R.D. Mountain and A.C. Brown, *J. Chem. Phys.* 80 (1984) 2730.
S. Nosé and F. Yonezawa, *J. Chem. Phys.* 84 (1986) 1803.
M.S. Watanabe and K. Tsumuraya, *J. Chem. Phys.* 87 (1987) 4891.
J.D. Honeycutt and H.C. Andersen, *J. Phys. Chem.* 91 (1987) 4950.
M.O. Robbins, K. Kremer and G.S. Grest, *J. Chem. Phys.* 88 (1988) 3286.
- [4] M.J. Mandell, J.P. McTague and A. Rahman, *J. Chem. Phys.* 64 (1976) 3699; 66 (1977) 3070.
C.S. Hsu and A. Rahman, *J. Chem. Phys.* 70 (1979) 5234; 71 (1979) 4974.
- [5] A. Stroobants, H.N.W. Lekkerkerker and D. Frenkel, *Phys. Rev. A* 36 (1987) 2929.
- [6] J.D. Honeycutt and H.C. Andersen, *Chem. Phys. Lett.* 108 (1984) 535; *J. Phys. Chem.* 90 (1986) 1585.
- [7] See e.g. D. Frenkel and J.F. Maguire, *Mol. Phys.* 58 (1983) 615.
- [8] B. Mulder, *Phys. Rev. A* 35 (1987) 3095.
- [9] W.G. Hoover and F.H. Ree, *J. Chem. Phys.* 49 (1968) 3609.
- [10] C.A. Angell, J.H.R. Clarke and L.V. Woodcock, *Adv. Chem. Phys.* 48 (1981) 398.
- [11] D. Frenkel, *Mol. Phys.* 60 (1987) 1.